Single-Crystal Resonance Raman Spectroscopy of Site-Directed Mutants of Cytochrome *c* Peroxidase†

Giulietta Smulevich,*,‡ Yang Wang,§ J. Matthew Mauro,∥ Jimin Wang,∥,⊥ Laurence A. Fishel,∥ Joseph Kraut,∥ and Thomas G. Spiro*,§

Dipartimento di Chimica, Università di Firenze, Via G. Capponi 9, 50121 Firenze, Italy, Department of Chemistry, Princeton University, Princeton, New Jersey 08544-1009, and Department of Chemistry, University of California at San Diego, La Jolla, California 92093

Received December 27, 1989; Revised Manuscript Received March 29, 1990

ABSTRACT: Resonance Raman spectra are reported for single crystals of cytochrome *c* peroxidase (CCP) mutants, taken by using a microscope equipped with a variable-temperature stage. The spectra are similar to those observed for the mutant proteins in solution, but there are detectable differences having to do with the coordination and spin state of the heme. The Asn-235 mutant contains a mixture of six-coordinate high- and low-spin states with a detectably higher fraction of the former than in solution. Upon cooling even to 223 K, the heme is converted mostly to the low-spin form. The Phe-191 mutant likewise shows a high/low-spin six-coordinate mixture, together with a preponderant population of five-coordinate heme. Upon cooling, the high-spin six-coordinate population converts immediately to the low-spin form, while the five-coordinate population does so more slowly. This behavior is intermediate between that of native CCP and the Asn-235 mutant, consistent with an ancillary role for the normal Trp-191–Asp-235 H-bond in the proximal anchoring of the heme Fe. The Phe-51 mutant shows a dominant high-spin five-coordinate heme population in the single crystal, whereas in solution the six-coordinate form is dominant. This difference is mimicked by adding 2-methyl-2,4-pentanediol (MPD) to the solution and is attributed to the dehydrating effect of MPD, which is present during crystallization. Upon lowering the temperature, the five-coordinate heme converts partially to a six-coordinate high-spin form. This mutant, as well as an aged form of native CCP, is unique in having a stable high-spin six-coordinate heme at low temperature. The spectra show selective orientation and polarization effects on the Raman band intensities, which can be understood quantitatively on the basis of the heme orientation relative to the crystal axes (oriented gas model). These effects help to discriminate among bands arising from vibrational modes of different symmetry, and they give information about the localization of the heme electronic transition moments in the protein.

Site-directed mutagenesis is providing valuable information about molecular interactions at the active site of cytochrome c peroxidase (CCP) (Mauro et al., 1989; Smulevich et al., 1988a,b). This enzyme catalyzes the reduction of hydrogen peroxide by cytochrome *c* (Yonetani, 1976). Attention naturally focuses on the factors promoting the cleavage of the peroxide O–O bond, a process of great biochemical significance. High-resolution crystal structures are available for CCP from bakers' yeast (Poulos et al., 1980; Finzel et al., 1984), and reveal a number of residues in the heme-binding pocket, which are poised to interact with the axial ligands of the heme Fe atom. Site-directed mutagenesis makes it possible to evaluate these interactions by systematic alteration of the chemical nature of these side chains (Fishel et al., 1987; Mauro et al., 1988). We have utilized resonance Raman (RR) spectra of the heme group to monitor these interactions via bands that are known to be markers of the coordination and spin state or of the status of the axial ligands (Smulevich et al., 1986a,b, 1988a,b, 1989, 1990). What emerges from these studies is a picture of an Fe atom in a state of dynamic tension due to forces exerted on the axial ligands by H-bond interactions from both the proximal and distal sides.

X-ray structure determinations on single crystals of these mutants are in progress (Wang et al., 1990). In the present study we examine RR spectra of single crystals of three mutants, involving Asp-235 → Asn, Trp-191 → Phe, and Trp-51 → Phe substitutions, by using a Raman microprobe apparatus equipped with a variable-temperature stage (Smulevich et al., 1990). This technique permits comparison of the patterns in single crystals, for which atomic coordinates can be precisely determined, with the same molecules in solution. Because the RR spectrum is sensitive to bonding interactions of the chromophore, it can provide information about crystal–solution structural differences that may be functionally important. In the present study we find subtle crystal–solution differences, related, we believe, to the availability of a water molecule as a sixth ligand in the resting form of the enzyme. In addition, we find pronounced orientation effects on the intensities and polarizations and show that the depolarization ratios are calculable from the orientations of the heme groups in the crystal by use of an oriented gas model. Recently Champion and co-workers have reported oriented single-crystal RR measurements on myoglobin (Morikis et al., 1988; Sage et al., 1989).

Experimental Procedures

Single crystals of the CCP(MI) mutants (Fishel et al., 1987) were prepared by the vapor diffusion method. Aliquots (8 μL) of 10–15 mg/mL protein solutions in 0.1 M phosphate buffer, pH = 6.0 (and pH = 5.5 for Asn-235), were mixed with equal

† This work was supported by NIH Grant GM 33576 (to T.G.S.) and NATO Grant 86/0453 (to G.S. and T.G.S.).

* Authors to whom correspondence should be addressed.
‡ Università di Firenze.
§ Princeton University.
∥ University of California at San Diego.
⊥ Present address: Department of Molecular Biophysics and Biochemistry, Yale University, New Haven, CT 06511.

0006-2960/90/0429-7174$02.50/0 © 1990 American Chemical Society

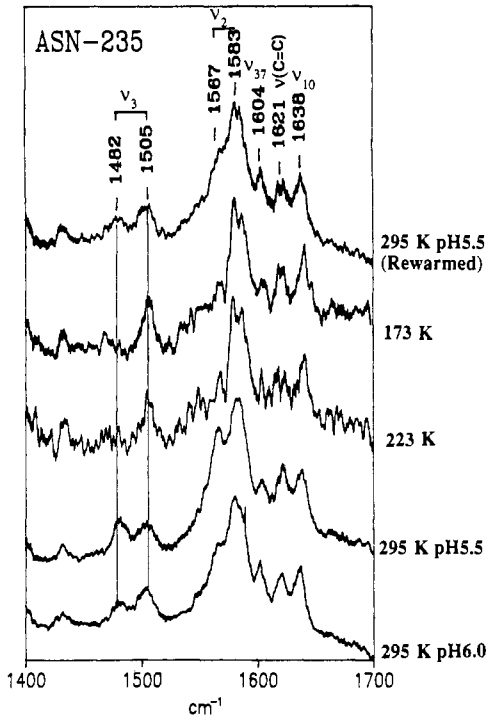

FIGURE 1: RR spectra (441.6-nm excitation) of Asn-235 CCP mutant single crystals grown from solution at pH 6.0 (bottom) and 5.5. Spectra of the latter were also obtained at 223 and 173 K and after rewarming to room temperature, 24 h later.

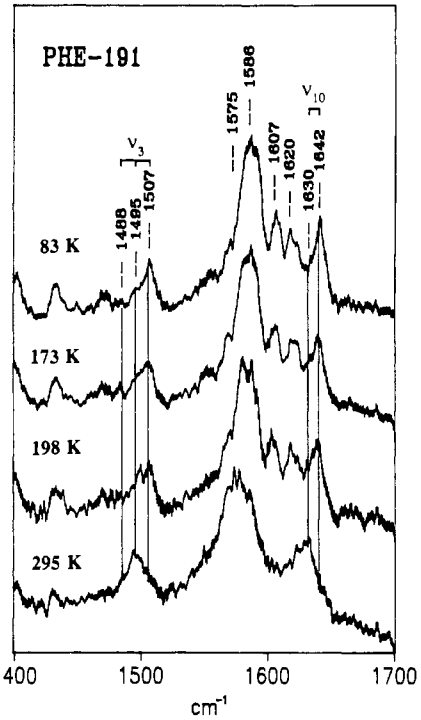

FIGURE 2: 441.6-nm-excited RR spectra of a Phe-191 mutant single crystal, at the indicated temperatures.

volumes of 40% 2-methyl-2,4-pentanediol (MPD) solution (v/v) and then equilibrated against reservoirs containing 30% MPD in sealed containers. Seeding with a small microcrystal in each drop usually produced a single large crystal in 3–7 days.

RR spectra were obtained in 180° backscattering from single crystals mounted on the stage of a Zeiss "Axioscope" microscope, which served as the foreoptics of a 0.75-m double spectrograph (Spex 1401 with the intermediate slit modified) equipped with 1200 g/mm gratings and a cooled reticon multichannel detector (Princeton Instruments). Details of the experimental arrangement have been described elsewhere (Smulevich et al., 1990). Laser damage (readily evident when the power was too high as irreversible photoreduction with the concomitant appearance of a black spot on the crystal) was avoided by attenuating the ~10-mW laser beam with a 1.5 OD neutral density filter and a polarizer (×4 attenuation). The laser flux at the crystal surface was estimated to be ~500 mW/mm^2 (spot size ~3 μm). For variable-temperature spectroscopy, the crystals were contained in a Joule–Thompson refrigerated sample holder mounted on the microscope stage. Solution spectra were obtained in the same apparatus with a capillary on the microscope stage; these spectra were checked against spinning-cell solution spectra and showed no differences.

Results

Asn-235. Figure 1 shows RR spectra with 441.6-nm excitation, near resonance with the Soret band, of a single crystal of the Asn-235 mutant of CCP. This mutation eliminates the H-bond between the proximal imidazole ligand (His-175) and the normal acceptor, Asp-235 (Finzel et al., 1984; see structural diagram, Figure 7), thereby allowing the Fe atom to move into the heme plane and bind the distal water molecule. The result is a six-coordinate (6-c) heme that is a mixture of high- and low-spin (h-s and l-s) states (Smulevich et al., 1988a). The spin and coordination state are monitored via the RR bands above 1450 cm^{-1} arising from skeletal modes of the porphyrin ring (Spiro & Li, 1988). The frequencies of these modes are sensitive to the porphyrin core size, which in turn responds to the spin and coordination state. The core size is at a minimum in the 6-c/l-s state and expands in the 6-c/h-s state because the antibonding $d_{x^2-y^2}$ orbital is partially occupied; it contracts to an intermediate value in the 5-c/h-s state when one of the axial ligands is lost and the iron is displaced from the heme plane (Spiro & Li, 1988). The position of the isolated ν_3 band is particularly characteristic: ~1505, ~1495, and ~1485 cm^{-1} for 6-c/l-s, 5-c/h-s, and 6-c/h-s states, respectively. The first and last of these bands are clearly seen in the Asn-235 spectra, and corresponding ν_2 bands (1583 and 1567 cm^{-1}) are also in evidence. Multiple components of the remaining core-size-sensitive modes are difficult to resolve because of band overlaps.

The crystal spectral pattern is similar to but not identical with that seen for Asn-235 in solution (Smulevich et al., 1988a). In both cases low pH favors the h-s over the l-s form, but in solution the former is a minority species even at pH 5, while the two forms have essentially equal ν_3 intensities at pH 5.5 in the single crystal. At low temperature the h-s form converts to the l-s form. Even at 223 K, hardly any high-spin form remains. Similar behavior is seen for frozen solutions of the Asn-235 mutant at 10 K, although addition of glycerol preserves the h-s fraction at low temperature (Smulevich et al., 1989). Warming the Asn-235 crystal regenerates the high/low-spin mixture but with a different ratio, indicating some irreversibility. For the Phe-191 and Phe-51 crystals, the temperature effects were completely reversible.

Phe-191. Figure 2 shows single-crystal RR spectra of the Phe-191 mutant. This mutation (Mauro et al., 1988) eliminates the H-bond between Trp-191 and Asp-235, part of the proximal-side anchoring chain of H-bonds (Wang et al., 1990; Finzel et al., 1984). Although the substitution has a profound effect on electron transfer activity (Mauro et al., 1988), presumably associated with the radical center of the ES intermediate being at Trp-191 (Sivaraja et al., 1989), the effect on ligation seems to be limited to allowing greater access to

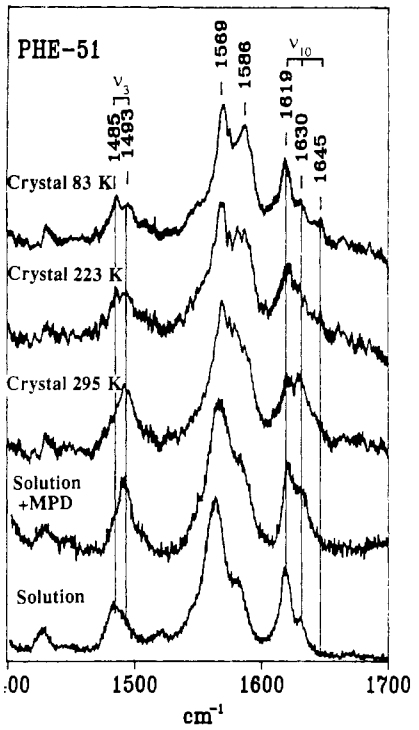

FIGURE 3: 441.6-nm-excited RR spectra of the Phe-51 mutant in pH 6 phosphate buffer (bottom) with 30% (v/v) MPD added. The top three spectra compare a Phe-51 single crystal at the indicated temperatures.

the distal water molecule, presumably by releasing some of the constraint on the Fe movement toward the heme plane. The result is a broad ν_3 band with dominant 5-c/h-s and lesser 6-c/h-s and 6-c/l-s contributions, whereas native CCP is purely 5-c/h-s (Smulevich et al., 1988a). As the temperature is lowered, the band envelope shifts toward a dominant 6-c/l-s component at 83 K. The evolution is complex, however, with the 6-c/h-s component (1486 cm^{-1}) being lost at 198 K but the 5-c/h-s (1495 cm^{-1}) component surviving to lower temperatures. This is just the behavior expected from interpolation of the characteristics shown by Asn-235 and native CCP. The former loses the 6-c/h-s form upon cooling to 223 K (Figure 1), while the latter has been shown to undergo a gradual conversion from 5-c/h-s to 6-c/l-s heme as the temperature is lowered, some 5-c contribution being present even at 83 K (Smulevich et al., 1989, 1990). Thus the Phe-191 mutant enzyme shows properties intermediate between native CCP and Asn-235, consistent with a secondary role for the affected proximal H-bond.

Phe-51. Figure 3 shows RR spectra of the Phe-51 mutant protein in a single crystal and also in solution. In this case there is a pronounced difference between crystal and solution spectra. The solution RR spectrum shows predominantly 6-c/h-s heme, as previously observed (Smulevich et al., 1988a), while the single crystal shows predominantly 5-c/h-s heme, consistent with the 2.7-Å distance between the Fe atom and the closest water molecule, W595, seen in the crystal structure (Wang et al., 1990). This difference is due to the 2-methyl-2,4-pentanediol (MPD) present in the crystallizing medium, since adding 30% MPD (the same concentration used for crystallization) to the Phe-51 solution results in conversion to a 5-c heme (Figure 3, bottom two spectra). Likewise, the addition of 50% or more glycerol to a solution of the Phe-51 mutant has been shown to convert the heme entirely to a 5-c form (Smulevich et al., 1989). We attribute this effect to the amphiphilic character of these additives. The Trp-51 → Phe mutation eliminates the H-bond from the Trp-51 residue (Finzel et al., 1984) to the distal water molecule, W595, which should therefore be less constrained than in CCP(MI). In the absence of additives, this loss of the constraining H-bond appears to permit coordination of W595 to the Fe. At the same time, the loss of the Trp-51 H-bond may permit the polyol additives to influence the distal H-bond network. The crystal structure, obtained with MPD present, shows W595 to be well ordered and H-bonded to both Arg-48 and His-52, interactions that are assisted by a small displacement, 0.3 Å, of these residues relative to CCP(MI). We infer that W595 is at a lower energy when bound to the Fe but that the presence of MPD tips the balance toward H-bonding with Arg-48 and His-52 at room temperature.

Lowering the temperature, however, tips the balance back toward binding to Fe, as evidenced by the growth in the 1485-cm^{-1} ν_3 component. No low-spin component is observed at low temperature, however, as was also demonstrated by EPR (Fishel et al., 1987). This behavior is in marked contrast to that of the Asn-235 mutant, for which the h-s → l-s conversion of the 6-c heme is complete at 223 K. In the case of bakers' yeast CCP, the heme is converted to a predominantly six-coordinate low-spin form at 83 K (Smulevich et al., 1990). If W595 is the sixth ligand in all these proteins, we infer that its ligand field is significantly weakened in the Phe-51 mutants. The source of this electronic effect is not obvious, but it probably relates to the nature of the distal H-bond network. It is also conceivable that the Trp-51 → Phe replacement affects the heme electronic state via altered π interactions with the porphyrin ring (Wang et al., 1990; Satterlee & Erman, 1983).

Glycerol was also found to influence the Asn-235 mutant, in this case increasing the fraction of 6-c/h-s relative to 6-c/l-s heme (Smulevich et al., 1989). Again the hydrophilic additive may affect the distal H-bond network, in this case weakening the Fe–water bond somewhat, thereby increasing the high-spin fraction. A similar effect of MPD might account for the slightly greater high-spin fraction seen in the Asn-235 single crystal relative to solution (see above).

Orientation Effects in Single-Crystal RR Spectra. Figure 4 shows RR spectra of the Phe-191 mutant for different orientations of the single crystal, which lies on its *ab* face on the microscope stage. The laser enters along the *c* direction, and the scattered light is collected in the reverse direction. The angles marked in Figure 4 refer to the angle of the laser electric vector relative to the *a* axis, which is the long axis of the crystal. The scattered light is analyzed into components that are perpendicular ($\perp$) and parallel ($\parallel$) to the incident electric vector. The $\perp/\parallel$ intensity ratio is the depolarization ratio, ρ. The value of ρ for the strong ν_4 band is given in the figure. Striking orientation effects are seen. The value of ρ doubles between 0° and 90° and doubles again at 45°. The 45° spectrum is clearly not intermediate between the 0° and 90° spectra. The bottom spectra in the figure were obtained in solution with the same experimental arrangement. The ρ value for ν_4, 0.11, is within experimental error of the expected isotropic value, 0.125, for an A_{1g} mode of a D_{4h} chromophore in resonance with an in-plane electronic transition (Spiro & Stein, 1977).

Figure 5 shows variable orientation spectra for the Asn-235 mutant, with 514.5-nm excitation, in resonance with the Q bands. At this wavelength nontotally symmetric modes, which are vibronically active, are enhanced (Spiro & Li, 1988). The dominant bands are the ν_{10} and ν_{11} (B_{1g}) and ν_{19} (A_{2g}) modes of the low-spin heme component. Again the orientation effects are dramatic. For B_{1g} modes the isotropic value of ρ is 0.75,

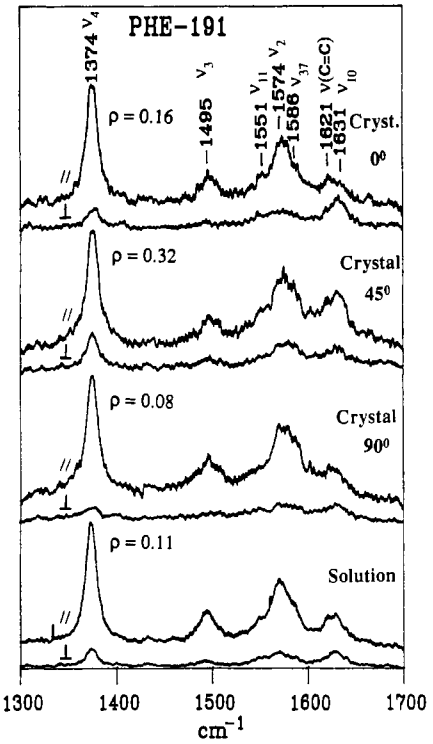

FIGURE 4: 441.6-nm-excited RR spectra, in parallel (∥) and perpendicular (⊥) scattering, for the Phe-191 mutant in solution (bottom) and in a single crystal with the laser electric vector aligned at 0°, 45°, and 90° to the long (*a*) axis of the crystal. The ρ values are the measured depolarization ratios (⊥/∥) for the ν_4 band.

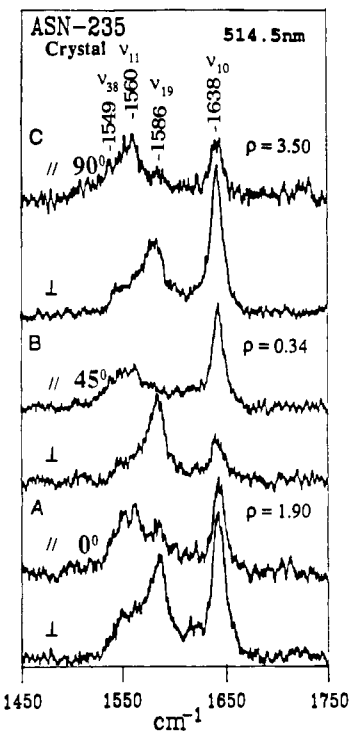

FIGURE 5: 514.5-nm-excited RR spectra, in parallel and perpendicular scattering, for an Asn-235 mutant single crystal, with the laser electric vector aligned at 0°, 45°, and 90° to the long (*a*) axis of the crystal. The ρ values are measured for the ν_{10} band.

but in the crystal ρ varies from 0.34 to 3.50 for the ν_{10} mode. Again the 45° value is not intermediate between the 0° and 90° values. A_{2g} modes are expected to appear only in the perpendicular spectra ($\rho = \infty$) in the crystal as well as in solution, due to their antisymmetric tensor (Spiro & Stein, 1977). The small ν_{19} component that can be seen in the

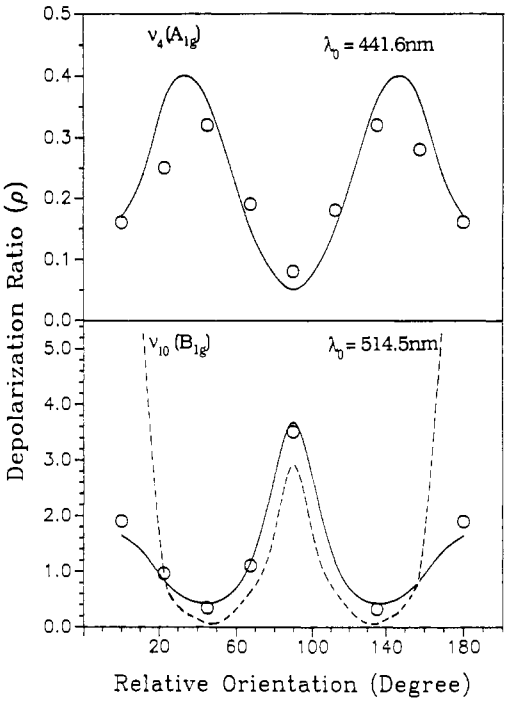

FIGURE 6: Plot of the single-crystal depolarization ratios (ρ) against angle of the electric vector relative to the *a* axis. Top: the ν_4 A_{1g} band (1374 cm^{-1}) of the Phe-191 mutant, excited at 441.6 nm. The solid line (—) represents the calculated ρ, by using χ = 106°; the open circles are the experimental data. Bottom: the ν_{10} B_{1g} band (1638 cm^{-1}) of the Asn-235 mutant excited at 514.5 nm. The solid line (—) represents the calculated ρ, by using χ = 128.5°; the dotted line (···) represents the calculated ρ, by using χ = 105°; the open circles are the experimental data.

Table I: Correlation Diagram for the Scattering Tensor Elements among the Molecular Site and Factor Groups

	D_{4h}	C_1	D_2	
$\alpha_{xx} + \alpha_{yy}$	A_{1g}	A	A	α_{aa}, α_{bb}, α_{cc}
$\alpha_{xx} - \alpha_{yy}$	B_{1g}	A	B_1	α_{ab}
$\alpha_{xy} + \alpha_{yx}$	A_{2g}	A	B_2	α_{ac}
$\alpha_{xy} - \alpha_{yx}$	B_{2g}	A	B_3	α_{bc}

parallel spectra is a reflection of the effective heme symmetry being somewhat lower than D_{4h}, due to the peripheral substituents and due to interactions with the protein.

The ρ variations are due to the symmetry properties of the normal mode scattering tensors and the disposition of the heme groups relative to the crystal axes. This subject has been discussed in detail by Sage et al. (1989) in connection with single-crystal RR spectra of myoglobin. The depolarization ratios can be calculated on the basis of the "oriented gas" model, in which intermolecular interactions of the chromophores are neglected. This is an excellent approximation for protein crystals, since the chromophores are well isolated from one another by the protein matrix. The proteins crystallize in the space group $P2_12_12_1$ (factor group D_2) with four molecules in general positions (Wang et al., 1990). The correlation of the scattering elements, α, between molecular axes (x, y, z) and crystal axes (a, b, c) is given in Table I for the in-plane Raman modes of a D_{4h} chromophore. The required geometric relationships involving the direction cosines of the crystal axes

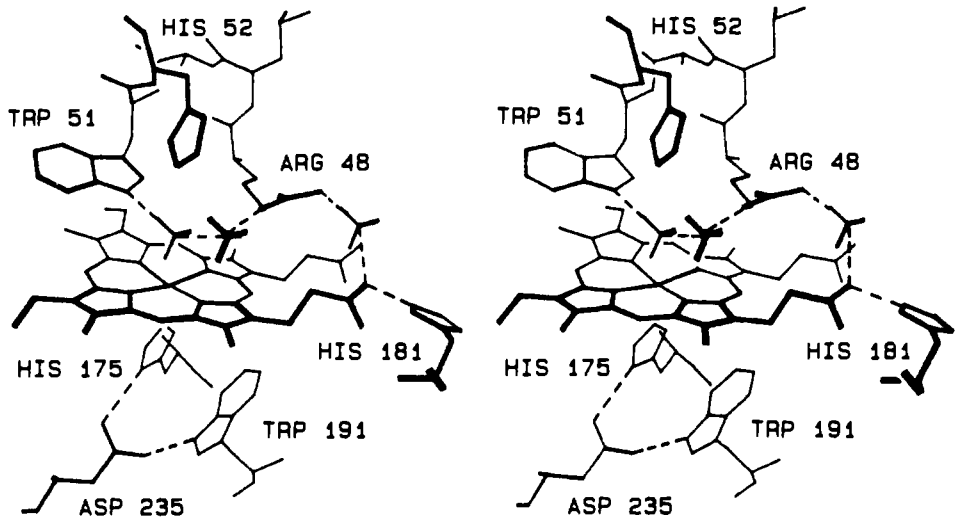

FIGURE 7: Heme crevice of ferric bakers' CCP from Finzel et al. (1984). Dotted lines indicate inferred hydrogen bonds, on the basis of distributed criteria. Three fixed water molecules are also shown.

Table II: Geometric Relations between Crystal and Heme (In-Plane) Tensor Elements in the *ab* Plane of CCP Mutant Crystals[a]

mode symmetry	α_{ij}	f_{ii}	$f_{i=j}$
A_{1g}	$f_{ij}(\alpha_{xx} + \alpha_{yy})$	$i_x^2 + i_y^2$	$i_xj_x + i_yj_y$
B_{1g}	$f_{ij}(\alpha_{xx} - \alpha_{yy})$	$i_x^2 - i_y^2$	$i_xj_x - i_yj_y$
B_{2g}	$f_{ij}\alpha_{xy}$	$2i_xi_y$	$i_xj_y + i_yj_x$
A_{2g}	$f_{ij}\alpha_{xy}$	$i_xi_y - i_yi_x = 0$	$i_xj_y - i_yj_x$

Direction Cosines as Functions of the Eulerian Angles[b]

$$a_x = \cos\gamma\cos\varphi\cos\chi - \sin\varphi\sin\chi$$
$$a_y = -\cos\gamma\cos\varphi\sin\chi - \sin\varphi\cos\chi$$
$$b_x = \cos\gamma\sin\varphi\cos\chi + \cos\varphi\sin\chi$$
$$b_y = -\cos\gamma\sin\varphi\sin\chi + \cos\varphi\cos\chi$$

[a] See Suzuki et al. (1968). [b] γ is the angle from the *c* crystal axis to the heme normal, *z*; φ is the angle from the *a* axis to the projection of *z* onto the *ab* plane; and χ is the angle in the heme plane, *xy*, between the *y* axis and the intersection of the heme plane, with the *ab* crystal plane.

Table III: Calculated[a] and Experimental[b] Depolarization Ratios for CCP Single Crystal Orientations[c]

	crystal orientation		0°	45°	90°
Phe-191	A_{1g}	calcd (χ = 106°)	0.17	0.36	0.05
	ν_4	exptl	0.16	0.32	0.08
	B_{1g}	calcd (χ = 105°)	52.6	0.06	2.19
	ν_{10}	exptl	1.90	0.34	3.5
Asn-235		calcd (χ = 128.5°)	1.64	0.42	3.67
	ν_{11}	exptl	1.15	0.88	1.00
		calcd (χ = 133°)	1.00	0.88	1.26

[a] Calculations based on D_{4h} symmetry and the geometric relations described in the text, with γ = 50.4°, φ = 21.32°, and χ = 106° for Phe-191 and γ = 51.5°, ψ = 23.8°, and χ = 105° for Asn-235 (Wang et al., 1990), or for the indicated χ values optimized to give the best agreement with experiment. [b] ν_4 measured with 441.6-nm excitation; ν_{11} and ν_{10} measured with 514.5-nm excitation. [c] Angle of the *a* crystal axis relative to the laser electric vector when the beam was directed along the normal to the 001 face.

with respect to the Eulerian angles describing the heme orientations are given in Table II (Wilson et al., 1980). For the geometry of the present experiment, in which the crystal *ab* face defines the tensor elements, the depolarization ratios at 0° and 90° to the *a* axis are $\rho_0 = \rho_a = \alpha^2_{ab}/\alpha^2_{aa}$; $\rho_{90°} = \rho_b = \alpha^2_{ab}/\alpha^2_{bb}$.

In Table III we compare the experimental ratios for ν_4 of the Phe-191 crystal, excited at 441.6 nm, and for ν_{10} and ν_{11} of the Asn-235 crystal, excited at 514.5 nm, with the values calculated on the basis of the heme orientations derived from the crystal structures (Wang et al., 1990). These crystals were selected because they gave the best signal/noise ratio with excitation in the B and Q band region, respectively. The agreement is very good for the ν_4 data but poor for the ν_{10} and ν_{11} data, as was also observed for bakers' yeast CCP crystals (Smulevich et al., 1990). We attribute this difference to the fact that the depolarization ratios of A_{1g} modes, which are totally symmetric, depend only on the orientation of the heme plane (defined by the angles γ and φ) and not on the directions of the *x* and *y* axes in the plane. The depolarization ratios of the B_{1g} modes, however, which are antisymmetric with respect to the *x*–*y* bisector (tensor pattern $\alpha_{xx} = -\alpha_{yy}$), are very sensitive to the *x*,*y* orientation in the plane, as determined by the angle χ.

In D_{4h} symmetry this orientation is arbitrary because the transition moments are isotropic in the plane of the chromophore. The *x* and *y* axes are conventionally taken as lying along the lines connecting the N atoms of the pyrrole rings,

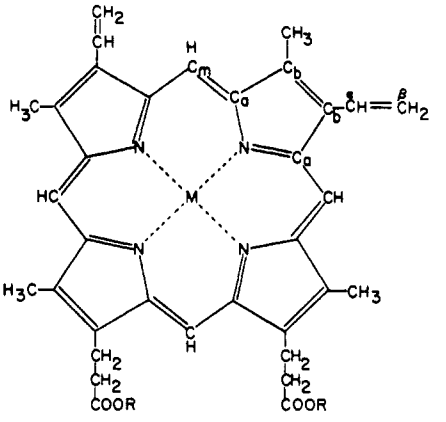

FIGURE 8: Structural diagram of protoheme (M = Fe). If the *x* and *y* axes are taken as the N–N directions, ν_{10} and ν_{11} classify as B_{1g} modes. They become B_{2g} if *x* and *y* are along the C_m–C_m directions.

with respect to which the B_{1g} eigenvectors are symmetric. It is this convention that was used in specifying χ from the crystal structure data. In the CCP mutant molecules, however, the in-plane transition moments are oriented by perturbations on the D_{4h} chromophores of the heme. These include the asymmetric disposition of the peripheral substituents, especially the vinyl groups of the protoheme (see Figure 8), electronic influences of the axial ligands, which are not 4-fold symmetric, and electrostatic interactions with surrounding protein residues. Consequently we allowed χ to vary and found, as in the case of bakers' yeast CCP (Smulevich et al., 1990), optimum values

that produced satisfactory agreement between calculated and measured depolarization ratios for each of the crystal orientations. The experimental values are somewhat uncertain for ν_{11} because of the weakness of this band (Figure 5) and its overlap with a nearby band, arising from an infrared mode, ν_{38} (Eu), which becomes activated by the influence of the vinyl groups (Choi et al., 1982). Despite the greater uncertainty, it is clear that the ν_{11} depolarization ratios are not the same as those of ν_{10}; they require a somewhat different optimized χ value for their calculation.

Discussion

Ligation and Spin State. These CCP mutants, whether in solution or in crystals, show a wide range of behavior with respect to coordination and spin state in the resting Fe(III) form. The RR spectra show the presence of five-coordinate high-spin and six-coordinate high- and low-spin heme in widely varying fractions. The fifth ligand is known to be the imidazole side chain of His-175. The sixth ligand is undoubtedly a water molecule at the pH value employed in this study. When the heme ligands are imidazole and water, the ligand field is close to the thermal spin crossover. The aquo complexes of methemoglobin and myoglobin are known to exist in a temperature-dependent mixture of high- and low-spin forms (Izuka & Kotani, 1969; Strekas & Spiro, 1974). At high pH, the sixth ligand is likely to be hydroxide, and indeed Terner and co-workers (Sitter et al., 1988) have established hydroxide coordination in resting horseradish peroxidase at high pH by identifying the Fe–OH stretch in the RR spectrum. We have previously attributed a small but distinct high pH shift in the ν_3 frequency of the low-spin heme fraction of the Asn-235 mutant with deprotonation of the water ligand (Smulevich et al., 1988a).

The RR spectra of the CCP mutants establish that both proximal and distal H-bonds play important roles in the balance of forces determining the coordination number and spin state. In native CCP the His-175 proximal imidazole donates an H-bond to the carboxylate group of Asp-235, which also accepts an H-bond from the indole ring of Trp-191 (Finzel et al., 1984; Wang et al., 1990). This H-bond chain probably constrains the movement of the Fe atom in the heme plane, and in addition the anionic character of His-175 resulting from the strong H-bond decreases the affinity for a sixth ligand; the heme group is five-coordinate. When the Asp-235 carboxylate is replaced by an amide group in the Asn-235 mutant, the H-bonding of His-175 is completely disrupted (Smulevich et al., 1988a), so that the steric and electronic constraints should both be relaxed. The result is tight binding of the distal water molecule to the Fe atom, forming a six-coordinate high/low-spin mixture. When the temperature is lowered, the entire population quickly converts to the low-spin form (223 K). The reorientation of the Trp-191 residue seen in the crystal structure (Wang et al., 1990) may also be relevant to this altered coordination behavior.

In the Phe-191 mutant, the Trp-191 → Asp-235 H-bond is lost, but otherwise the main structural consequence is a small compression of the proximal domain of the polypeptide chain toward the heme (Wang et al., 1990). The RR spectrum shows some six-coordinate species, both low and high spin, although the predominant form is five-coordinate, both in crystals and in solution. Lowering the temperature quickly converts the six-coordinate population entirely to the low-spin form, just as in the Asn-235 mutant. But the five-coordinate population persists and is converted to the six-coordinate low-spin form only gradually at much lower temperature. This behavior of the five-coordinate fraction is the same as observed previously for bakers' yeast CCP (Smulevich et al., 1990). Thus the Phe-191 mutant shows a heterogeneous heme population and behaves as if it were a mixture of native CCP and the Asn-235 mutant. This behavior is consistent with the view that the Trp-191 → Phe substitution allows the Fe greater freedom to approach the heme plane and bind W595.

Quite different behavior is found for the H-bond between the Trp-51 residue and the distal water molecule. When this H-bond is lost by substituting Phe for Trp, a predominantly six-coordinate high-spin heme population is formed in solution but not in the crystal, which remains five-coordinate. This difference can be traced to the presence of MPD in the crystallizing medium, which is presumed to influence the distal H-bond network by virtue of its hydrophillic character and thereby shift the energy balance toward W595 being H-bonded to the distal residues Arg-48 and His-52, at a distance from the Fe sufficient to prevent coordination. This effect is overcome at low temperature, however, where W595 becomes bound to the Fe, as it is at room temperature in the absence of polyalcohol additives. The ground state of the aquo complex in the Phe-51 protein is high spin, however, in contrast to the situation of CCP(MI) and other mutants in which Trp-51–W595 H-bonding is available, for which the ground state is low spin. This difference is also presumed to originate in the details of the distal H-bond network.

Orientation and Polarization Effects. It is satisfying that the single-crystal RR depolarization ratios can be quantitatively understood on the basis of the oriented gas model by using the crystal structure and D_{4h} symmetry rules. These rules had to be relaxed only to the extent of allowing χ to vary in the case of nontotally symmetric modes, from the angle calculated on the basis of the N–N directions. The required χ rotations can be considered as mixing B_{2g} with B_{1g} character due to the symmetry lowering of the protoheme chromophore in the protein. In D_{4h} symmetry, the B_{2g} modes are symmetric with respect to the lines connecting the methine bridge atoms, C_m (Figure 8); their tensor elements are α_{xy}. A B_{2g} mode is calculated to have the same depolarization ratio as a B_{1g} mode when χ is rotated by 45°. Thus a combination of B_{2g} and B_{1g} character (α_{xy} as well as $\alpha_{xx} - \alpha_{yy}$ elements) can produce any χ value.

Other symmetry-lowering effects might be anticipated, including nonequivalent and nonorthogonal x and y transition moments, nonequivalent α_{xx} and α_{yy} enhancement due to x,y splitting in the excited state, and nonzero values of out-of-plane tensor elements α_{zz}, α_{xz}, or α_{yz}. The anticipated influences of some of these effects on the A_{1g} depolarization ratio have been considered by Sage et al. (1989). None of them seems to be important for the CCP mutants or for bakers' yeast CCP (Smulevich et al., 1990) in view of the successful D_{4h} calculation of the depolarization ratios, allowing only χ to vary for the nontotally symmetric modes. Not only are the ρ values satisfactorily calculated at the three orientations listed in Table III, but the entire crystal rotation dependence is well reproduced, as shown in Figure 6 for ν_4 of Phe-191 and ν_{10} of Asn-235. This high level of agreement implies the following: (a) The crystal is well-oriented. [We note that the ρ orientation curve of the Mb ν_4 band was found by Sage et al. (1989) to be shifted relative to the calculated curve, an effect attributed by them to crystal misalignment; it seems likely that the microscope stage provides for more reliable alignment than the optical arrangement described by Sage et al., which involved front scattering from a crystal mounted at an angle of 18.5° to the laser beam.] (b) $\alpha_{xx} = \alpha_{yy}$ (A_{1g}) or $\alpha_{xx} = -\alpha_{yy}$ (B_{1g}). (c) Out-of-plane tensor elements are negligible. Thus

the only detectable effect of symmetry lowering is the steering of the in-plane electronic transition moments. Steering of the electronic transition moment appears to be different for the Asn-235 mutant and for bakers' yeast CCP if we compare the optimum χ for an isolated B_{1g} mode, in order to avoid the complicating effects of near-resonant interactions. For Asn-235, ν_{10} is well isolated, while for bakers' yeast CCP, ν_{11} is not overlapped (Smulevich et al., 1990). The χ value for the latter was found to deviate by 44° from the line of the pyrrole N atoms, while for ν_{10} of Asn-235 the deviation is 23° (Table III). Both structural and electronic alterations may be involved in this difference, since bakers' yeast CCP has a five-coordinate high-spin heme while Asn-235 has a (mainly) six-coordinate low-spin heme. This conversion involves a flattening of the porphyrin and movement of the Fe into the plane, while the electronic structure change alters the interaction of the Fe d orbitals with the resonant electronic transition.

We attribute the fact that the optimized χ differs somewhat for ν_{10} and ν_{11} (Table III) to a near-resonant interaction between ν_{11} and ν_{38} (which becomes allowed via the symmetry lowering). A similar interaction between ν_{10} and the vinyl C=C stretching mode in native CCP (this interaction is relieved in the Asn-235 mutant because of an upshift in the ν_{10} frequency due to the low-spin heme) was suggested to account for deviations in the optimal χ that was found to be required for these bands (Smulevich et al., 1990).

Acknowledgments

We are grateful to Professor Mario Marzocchi for his interest and guidance with respect to the tensor calculations.

References

Choi, S., Spiro, T. G., Langry, K. C., Smith, K. M., Budd, D. L., & LaMar, G. N. (1982) *J. Am. Chem. Soc. 104*, 4345.

Dasgupta, S., Rousseau, D. L., Anni, H., & Yonetani, T. (1989) *J. Biol. Chem. 264*, 654.

Edwards, S. L., Poulos, T. L., & Kraut, J. (1984) *J. Biol. Chem. 259*, 2976.

Evangelista-Kirkup , R., Crisanti, M., Poulos, T., & Spiro, T. G. (1985) *FEBS Lett. 192*, 2976.

Fishel, L. A., Villafranca, J. E., Mauro, J. M., & Kraut, J. (1987) *Biochemistry 26*, 351.

Finzel, B. C., Poulos, T. L., & Kraut, J. (1984) *J. Biol. Chem. 259*, 13027.

Hashimoto, S., Teraoka, J., Inubushi, T., Yonetani, T., & Kitagawa, T. (1986a) *Proc. Natl. Acad. Sci. U.S.A. 83*, 2617.

Hashimoto, S., Teraoka, J., Inubushi, T., Yonetani, T., & Kitagawa, T. (1986b) *J. Biol. Chem. 261*, 11110.

Iizuka, T., & Kotani, M. (1969) *Biochim. Biophys. Acta 194*, 351.

Mauro, J. M., Fishel, L. A., Hazzard, J. T., Meyers, T. E., Tollin, G., Cusanovich, M. A., & Kraut, J. (1988) *Biochemistry 27*, 6243.

Mauro, J. M., Miller, M. A., Edwards, S. L., Wang, J., Fishel, L. A., & Kraut, J. (1989) in *Metal Ions in Biological Systems* (Sigel, H., & Sigel, A., Eds.) Vol. 25, pp 477–503, Marcel Dekker, New York.

Morikis, D., Sage, J. T., Rizos, A. K., & Champion, P. M. (1988) *J. Am. Chem. Soc. 110*, 6341.

Poulos, T. L., Freer, S. T., Alden, R. A., Edwards, S. L., Skogland, U., Takio, K., Eriksson, B., Xuong, N., Yonetani, T., & Kraut, J. (1980) *J. Biol. Chem. 255*, 575.

Sage, J. T., Morikis, D., & Champion, P. M. (1989) *J. Chem. Phys. 90*, 3015–3032.

Satterlee, J. D., & Erman, J. E. (1983) *J. Biol. Chem. 258*, 1050.

Sitter, A. J., Shifflett, J. R., & Terner, J. (1988) *International Conference on Raman Spectroscopy* (Clark, R. J. H., & Long, D. A., Eds.) pp 659–660, John Wiley & Sons, Chichester, U.K.

Sivaraja, M., Goodin, D. B., Mauk, A. G., Smith, M., & Hoffman, B. M. (1989) *Science 245*, 738–740.

Smulevich, G., Evangelista-Kirkup, R., English, A., & Spiro, T. G. (1986a) *Biochemistry 25*, 4426.

Smulevich, G., Dasgupta, S., English, A., & Spiro, T. G. (1986b) *Biochim. Biophys. Acta 873*, 88.

Smulevich, G., Mauro, J. M., Fishel, L. A., English, A. M., Kraut, J., & Spiro, T. G. (1988a) *Biochemistry 27*, 5477–5485.

Smulevich, G., Mauro, J. M., Fishel, L. A., English, A. M., Kraut, J., & Spiro, T. G. (1988b) *Biochemistry 27*, 5486–5492.

Smulevich, G., Mantini, A. R., English, A. M., & Mauro, J. M. (1989) *Biochemistry 28*, 5058.

Smulevich, G., Wang, Y., Edwards, S., Poulos, T., English, A. M., & Spiro, T. G. (1990) *Biochemistry 29*, 2586.

Spiro, T. G., & Stein, P. (1977) *Annu. Rev. Phys. Chem. 28*, 501.

Spiro, T. G., & Li, X.-Y. (1988) in *Biological Applications of Raman Spectroscopy* (Spiro, T. G., Ed.) Vol. 3, p 1, John Wiley & Sons, New York.

Strekas, T. C., & Spiro, T. G. (1974) *Biochim. Biophys. Acta 351*, 237.

Suzuki, M., Yokoyama, T., & Ito, M. (1968) *Spectrochim. Acta 26A*, 1091.

Wang, J., Mauro, M. J., Fishel, L. A., Edwards, S. L., Oatley, S. J., Ashford, V. A., Xuong, N., & Kraut, J. (1990) *Biochemistry* (preceding paper in this issue).

Wilson, E. B., Jr., Decius, J. C., & Gross, P. C. (1980) *Molecular Vibrations: The Theory of Infrared and Raman Vibrational Spectra*, Dover Publications, Inc., New York.

Yonetani, T., & Anni, H. (1987) *J. Biol. Chem. 262*, 9547.